Hindawi Publishing Corporation
International Journal of Photoenergy
Volume 2014, Article ID 586707, 12 pages
http://dx.doi.org/10.1155/2014/586707

Research Article

Surface Modification of Aerosol-Assisted CVD Produced TiO_2 Thin Film for Dye Sensitised Solar Cell

SuPei Lim,[1] Nay Ming Huang,[1] Hong Ngee Lim,[2,3] and M. Mazhar[4]

[1] *Low Dimensional Materials Research Centre, Department of Physics, Faculty of Science, University of Malaya, 50603 Kuala Lumpur, Malaysia*
[2] *Department of Chemistry, Faculty of Science, Universiti Putra Malaysia, 43400 Serdang, Selangor, Malaysia*
[3] *Functional Device Laboratory, Institute of Advanced Technology, Universiti Putra Malaysia, 43400 Serdang, Selangor, Malaysia*
[4] *Department of Chemistry, Faculty of Science, University of Malaya, 50603 Kuala Lumpur, Malaysia*

Correspondence should be addressed to Nay Ming Huang; huangnayming@gmail.com
and Hong Ngee Lim; hongngee@upm.edu.my

Received 16 August 2013; Accepted 14 November 2013; Published 5 February 2014

Academic Editor: Věra Cimrová

We report a simple and convenient method for the preparation of Ag/TiO_2 thin films supported on indium tin oxide, which was achieved by sonochemical deposition of Ag^+ on aerosol-assisted chemical vapour deposited TiO_2 thin films. Posttreatment was performed on the film by immersion in HCl. The as-prepared composite film was characterised by X-ray diffraction, ultraviolet-visible absorption spectroscopy, Raman spectroscopy, and field emission scanning electron microscopy. The photoelectrochemical measurements and *J-V* characterisation showed approximately fivefold increase in photocurrent density generation and approximately sevenfold enhancement in dye sensitiser solar cell (DSSC) conversion efficiency, which was achieved after modification of the TiO_2 film with HCl posttreatment and Ag particle deposition. The improved photocurrent density of 933.30 $\mu A/cm^2$, as well as DSSC power conversion efficiency of 3.63% with high stability, is an indication that the as-synthesised thin film is a potential candidate for solar energy conversion applications.

1. Introduction

For decades, titanium dioxide has been substantially researched and has a wide range of applications including solar cells [1], environmental purification [2, 3], gas sensing [4, 5], water photolysis [4, 6], and biomedical devices [7, 8]. The large scope of applications is due to the excellent functionality, low cost, and stability of TiO_2 in most environments [6, 9]. In addition, since the discovery of dye sensitised solar cells (DSSCs) by O'Regan and Grätzel in 1991 [10], DSSCs have attracted vast academic and industrial interest due to their high power conversion efficiency, low cost, and ease of fabrication.

The basic concept of the DSSC involves using the highly porous TiO_2 thin film as a photoanode, allowing a large amount of sensitising organic dye to be adsorbed. The adsorbed dye will absorb light and photoexcited electrons will transfer to the conduction band of TiO_2. Following this, the dye is regenerated by I^-/I^{3-} [10, 11] through diffusion of electrons to the counter electrode. Thus, high solar conversion efficiency in DSSCs requires not only a large surface area of porous TiO_2, for a large amount of dye adsorption, but also optimum construction or good networking between particles for light harvesting and fast electron transportation [12–15].

Many methods have been reported for the preparation of TiO_2 photoanodes including sol-gel hydrothermal synthesis method [16, 17]; the electrospinning technique [18]; sol-gel [19, 20]; the hydrothermal method [21]; the anodisation/electrodeposition method [1, 22]; the screen printing method [23, 24]. However, to the best of our knowledge,

there has not been a study on TiO_2 photoanodes for DSSC applications fabricated by aerosol-assisted chemical vapour deposition (AACVD).

Despite many advantages of the AACVD method including simple set-up, low maintenance, and low set-up costs, the method has not previously been utilised for the preparation of TiO_2 thin films for DSSC photoanodes. This could be due to the difficulties of controlling the characteristics, such as the porosity, of the produced TiO_2 thin films. Poor porosity will limit the dye adsorption and affect the transportation of electrons in the DSSC system. Hence, it is important to devise a way to fabricate an efficient DSSC using the AACVD method. In this report, we propose posttreatment of the TiO_2 thin film with HCl, followed by surface modification with silver.

We report, for the first time, performance studies of DSSCs containing a TiO_2 thin film prepared by the AACVD method. Photoelectrochemical properties and DSSC performance of the hybrid film were greatly increased following HCl posttreatment and Ag inclusion.

2. Experimental

2.1. Materials. Titanium isopropoxide (TTIP, 98%) was purchased from Acros Organics. Methanol and HCl were purchased from Systerm. Silver nitrate ($AgNO_3$) was purchased from Merck. Indium tin oxide (ITO) conducting glass slides (7 Ω/sq.) were commercially supplied by Xin Yan Technology Limited, China. Deionised water was used throughout sample preparation.

2.2. Deposition of TiO_2 Thin Film by AACVD. TiO_2 thin films were prepared on the ITO substrates (1 × 1.5 cm) using the in-house AACVD assembly previously described [2]. The ITO substrates were ultrasonically cleaned with acetone, 1 M NaOH solution, and deionised water. TTIP was added to methanol to obtain a 0.1 M solution, and the solution was used to generate an aerosol at room temperature using an ultrasonic air humidifier operating at 60 Hz. Argon gas was passed through the aerosol mist at a flow rate of 200 mL/min to carry the aerosol droplets into the reactor chamber. Depositions were conducted at 450°C for 90 min. The exhaust from the reactor was vented directly into the extraction system of the fume cupboard. The aerosol line was closed toward the end of the experiment and pure argon was allowed to flow. The film was then cooled and stored in air.

2.3. Posttreatment of TiO_2 Thin Film. Posttreatment of the TiO_2 thin films (P-TiO_2) was carried out by immersing the films in 0.1 M HCl. After 30 min, the film was removed from the HCl solution. The film was rinsed with deionised water and dried in an oven at 60°C.

2.4. Preparation of Ag-Loaded TiO_2 Thin Film. To obtain the Ag-loaded TiO_2 thin films Ag/TiO_2 and P-Ag/TiO_2, samples TiO_2 and P-TiO_2 were immersed in 0.001–0.01 M $AgNO_3$ aqueous solution and stimulated using an ultrasonic generator (Kudos) at a frequency of 50 kHz for 30 min. The film was then washed with deionised water and dried in air.

2.5. Fabrication of Dye Sensitised TiO_2 and Ag/TiO_2 Films with and without Posttreatment. The films were immersed in an ethanol solution of 0.3 mM N719 (Ruthenizer 535-bisTBA, Solaronix) dye for 24 h. After sensitisation, the film was washed with ethanol. The dye absorbed electrode was assembled into a sandwich-type cell with a counter electrode (platinum-sputtered ITO glass). The counter electrode and dye sensitised TiO_2 electrode were clamped firmly together, and redox electrolyte (Iodolyte Z-100, Solaronix) solution was introduced into the dye sensitised electrode by capillary action. An active area of 0.5 cm^2 was used to measure the cell performance.

2.6. Characterisation. The crystalline phase of the samples was determined via X-ray diffraction XRD (D5000, Siemens), using copper Kα radiation (λ = 1.5418 Å) at a scan rate of 0.02 degrees s^{-1}. The morphology of the Ag/TiO_2 thin film was examined using field emission scanning electron microscopy FESEM (FEI Nova NanoSEM 400, operated at 10.0 kV). Optical absorption properties in the spectral region 190–900 nm were assessed using a UV-Vis spectrophotometer (Thermo Scientific Evolution 300). Raman spectra were collected using a Renishaw 2000 system with an argon ion laser emitting at 514.5 nm.

2.7. Cyclic Voltammetry. Electrochemical characterisation, to obtain linear sweep voltammetry (LSV) plots and chronoamperometry plots, was performed in the three-electrode VersaSTAT 3 electrochemical analyser from Princeton Applied Research. The system was equipped with an electrochemical cell consisting of Ag/AgCl (in 3 M NaCl) as the reference electrode and a platinum wire as the counter electrode. 0.5 M KCl was employed as a supporting electrolyte. The time dependence of the photocurrent was obtained under illumination from a 150 W Xenon arc lamp (Newport, model 69907), using an AM1.5G filter with a manual shutter.

2.8. DSSC Conversion Efficiency Measurement. The photovoltaic performance of the DSSCs was recorded using the VersaSTAT 3 electrochemical analyser from Princeton Applied Research. A 150 W Xenon arc lamp simulated solar illumination with the use of an AM1.5G filter. The intensity of illumination, measured using a fiber optic spectrometer (Avaspec-2048), was 20 mW/cm^2.

3. Results and Discussion

By analysis of XRD patterns (Figure 1), it is observed that most of the peaks caused by the ITO glass slide are no longer visible after the AACVD process, indicating successful deposition of TiO_2 onto the ITO glass slide (Figure 1(a)). The TiO_2 films, TiO_2 and P-TiO_2 (Figures 1(b) and 1(d)), are composed of mixed anatase and rutile phases, which agrees with reference patterns JCPDS 83-2243 and 21-1276, respectively. The diffraction peak at 25.3° corresponds to the

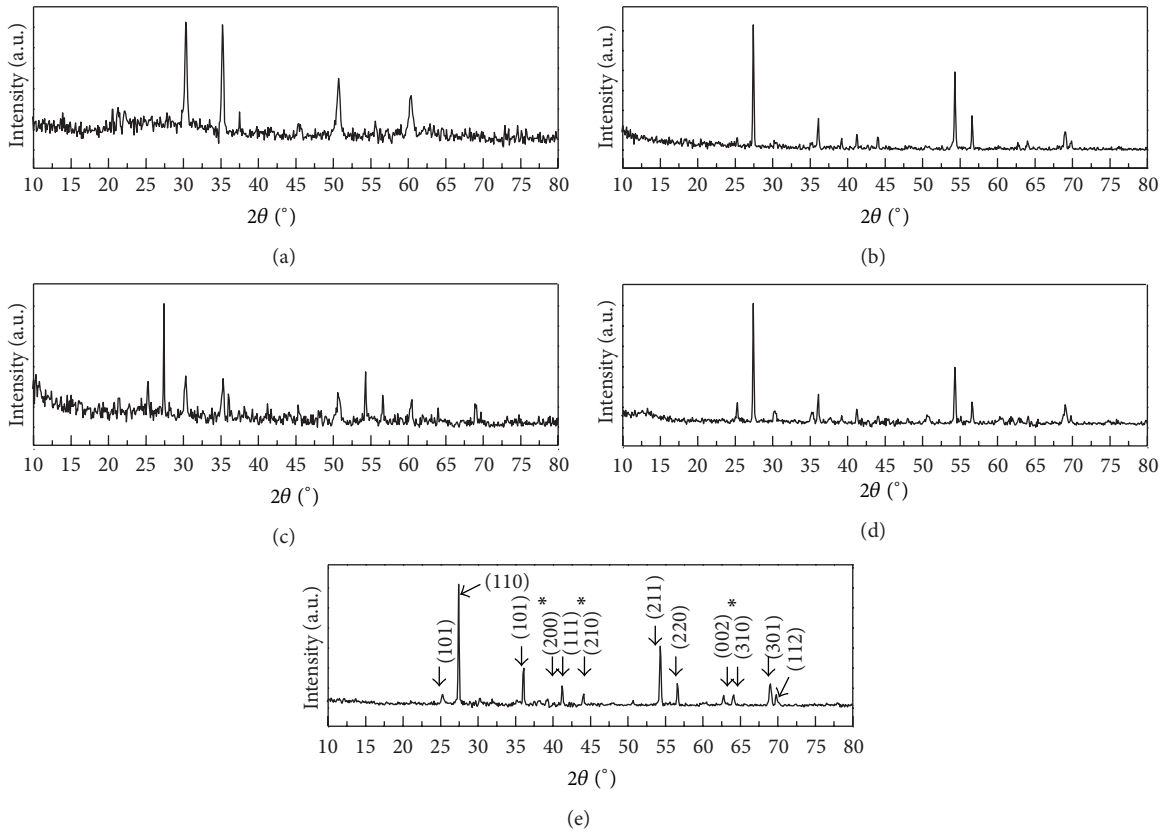

Figure 1: X-ray diffraction patterns of (a) ITO; (b) TiO_2; (c) Ag/TiO_2; (d) P-TiO_2; (e) P-Ag/TiO_2.

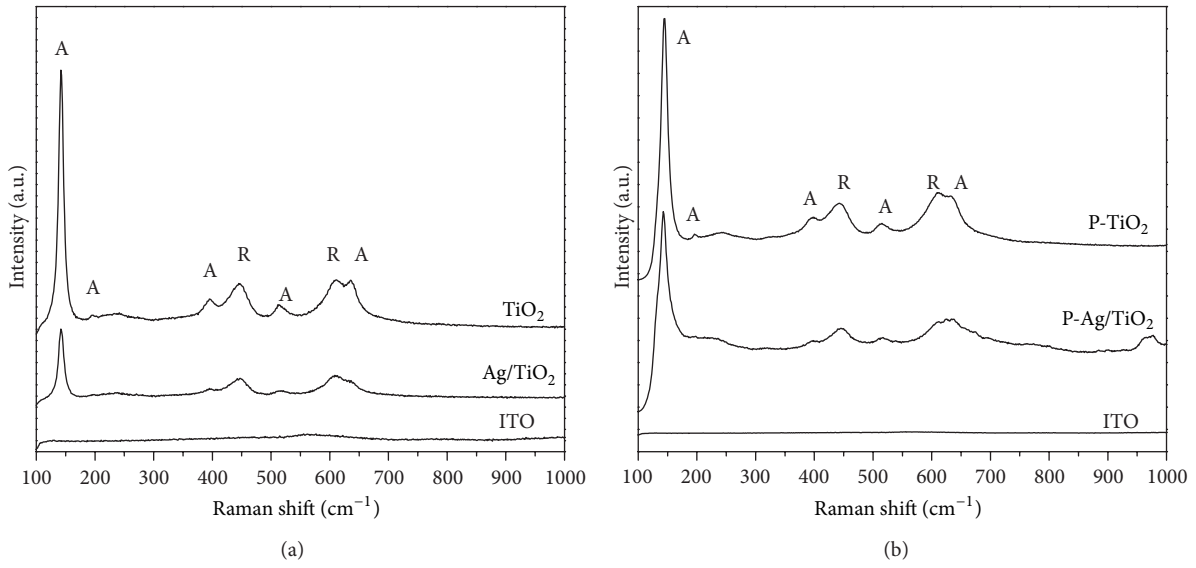

Figure 2: Raman spectra for (a) ITO, Ag/TiO_2, and TiO_2; (b) ITO, P-Ag/TiO_2, and P-TiO_2.

anatase phase of TiO_2. The peaks at 27.4°, 36°, 39.1°, 41.2°, 44.1°, 54.3°, 56.7°, 62.74°, 64.1°, 68.9°, and 70° agree well with the rutile phase of TiO_2. The diffraction peaks corresponding to (200), (210), and (310) peaks of TiO_2 are very close to the peaks of Ag (JCPDS 41-1104) at (111), (200), and (220). It is therefore difficult to differentiate the Ag signals from the TiO_2 signals due to the low Ag content in Ag/TiO_2 and P-Ag/TiO_2 (Figures 1(c) and 1(e)).

To further evaluate the phases in the prepared films, Raman spectroscopy was performed in the range 100–1000 cm^{-1}, and the results are shown in Figures 2(a) and 2(b). The anatase TiO_2 phase was observed at 143, 194, 398, 512,

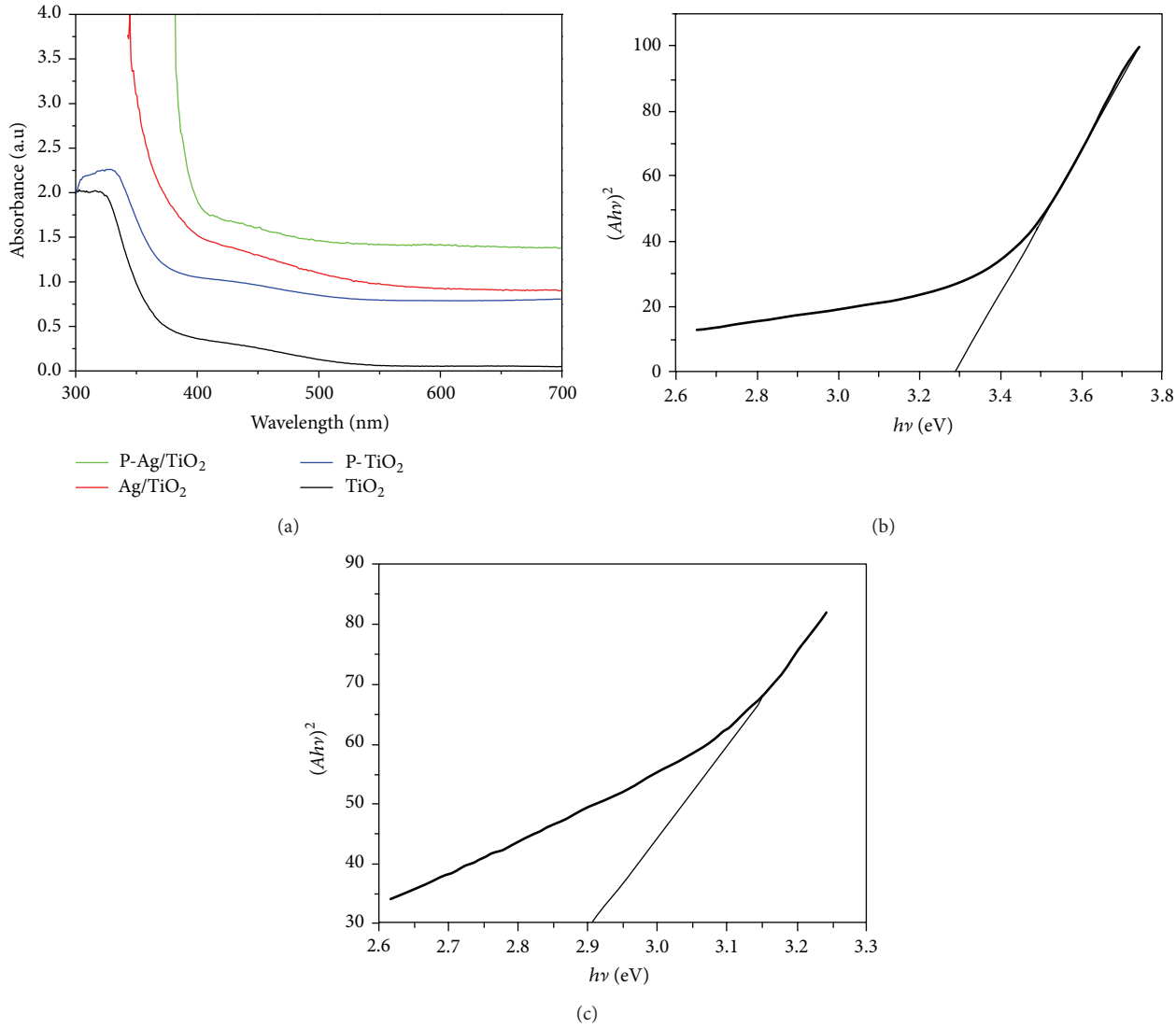

Figure 3: (a) UV-Vis spectra for TiO_2, Ag/TiO_2, $P\text{-}TiO_2$, and $P\text{-}Ag/TiO_2$. Band gap estimation for (b) TiO_2 and (c) Ag/TiO_2.

and 632 cm^{-1}. The rutile TiO_2 phase was detected at 449 and 611 cm^{-1}. However, signals related to Ag particles were not identified for samples with and without HCl posttreatment, due to the relatively low concentration of Ag loaded onto the TiO_2 thin film and its weak Raman scattering power [25]. An interesting observation is that the peak intensities are reduced with deposition of Ag, but the position of the peaks remains the same. This indicates that there is an interaction between Ag and TiO_2 that affects the Raman resonance of TiO_2 [26].

The UV-Vis spectra of the thin films are shown in Figure 3(a). It can be clearly seen that the addition of Ag onto TiO_2 caused a red shift of the wavelength. This has the effect of lowering the band gap energy of TiO_2. An estimation of the band gap energy (eV) was determined using a Tauc plot [$(Ah\nu)^n$ versus $h\nu$], where A is a constant, n is the power of the exponent ($n = 2$ for a direct allowed transition and $n = 1/2$ for an indirect allowed transition), and $h\nu$ is the incident photon energy. The resulting plots of direct allowed transitions, with an extrapolation to the x-axis, for TiO_2 and Ag/TiO_2 are shown in Figures 3(b) and 3(c). The band gap energy of TiO_2 decreased from 3.29 eV to 2.90 eV following deposition of Ag. Some studies report that the presence of Ag on a TiO_2 thin film results in more excitation due to surface plasmon resonance [27–29]. Moreover, Ag assists in reducing the band gap energy and retarding the charge recombination [25, 28, 30]. These improvements directly enhance the photocurrent. Modification of the TiO_2 thin film has possible applications in dye sensitised solar cells (DSSCs) [31–33], photocatalysts [34], hydrogen production [35], and sensing [36, 37].

The mechanism for the growth of Ag on the TiO_2 surface is illustrated in Figure 4(a). The sonochemical growth of Ag particles consists of two steps: nucleation and growth. In the nucleation step, the TiO_2 acts as the seed for the Ag particle. The collapse of the bubbles induced by the sonication

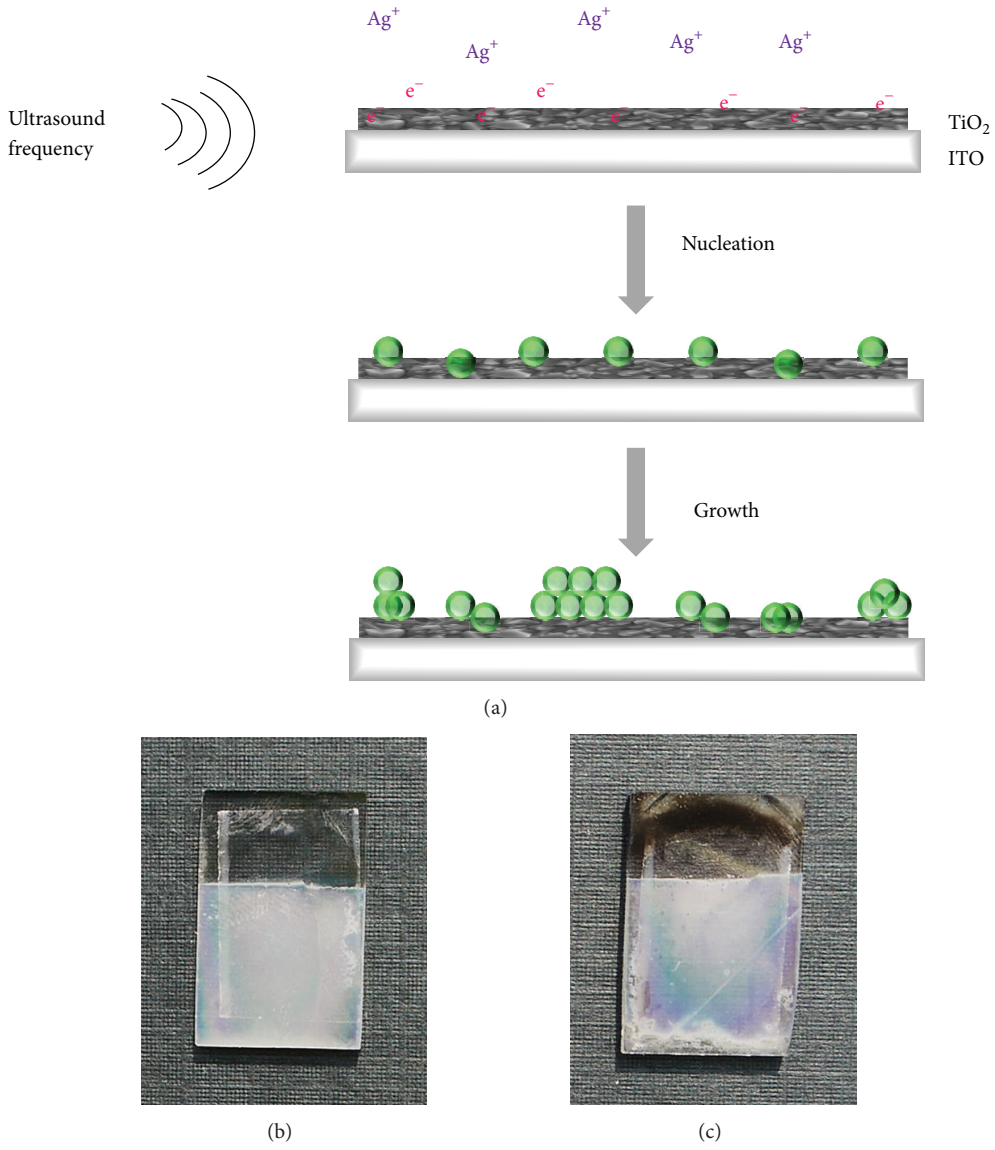

Figure 4: (a) Schematic of the mechanism for the growth of Ag on TiO_2. Physical appearance of (b) TiO_2 and (c) Ag/TiO_2.

process will result in high energy, exciting the electrons in the conduction band of TiO_2 crystals [38]. The generated electrons will accumulate on the surface of TiO_2 and attract the positively charged Ag^+ due to the electrostatic interaction between the oppositely charged ions. The Ag^+ ion is then reduced to an Ag particle. As the sonication process proceeds, the excited electrons will be generated continuously. The Ag seed will act as electron storage and attract more Ag^+, hence the growth of Ag particles. The TiO_2 and Ag/TiO_2 films are shown in Figures 4(b) and 4(c). The physical appearance of the films on the ITO glass is translucent. The thicknesses of the as-deposited films are fairly uniform between 600 and 700 nm, measured using a surface profiler. The TiO_2 films are strongly attached to the ITO glass, as they are able to endure the Scotch tape test. They also resist common solvents and do not dissolve in 1 M HCl or 1 M NaOH solutions.

The microscopic morphology of the thin films was studied using FESEM. Figures 5(a) and 5(b) show images of pure TiO_2 and TiO_2 with HCl posttreatment, respectively. The post-treated film appears pyramidal. Figures 5(c) and 5(d) show images of the Ag/TiO_2 film, with 0.005 M Ag concentration, with and without HCl posttreatment. Interestingly, after the addition of Ag, the microstructure of TiO_2, which initially appears pyramid-like, changes significantly to consist of numerous nanoparticles resembling stone blocks, attached to the pyramidal structure. No significant changes in morphology were observed for the film with and without HCl posttreatment. The presence of Ag on TiO_2 was confirmed by EDX analysis, as shown in Figures 5(e) and 5(f). The untreated Ag/TiO_2 thin film contains not only Ti, O, Ag, and C, but also Na. This implies that some chemical reactions occur at the glass substrate/thin film interface, and that sodium ions migrate from the glass substrate into the thin

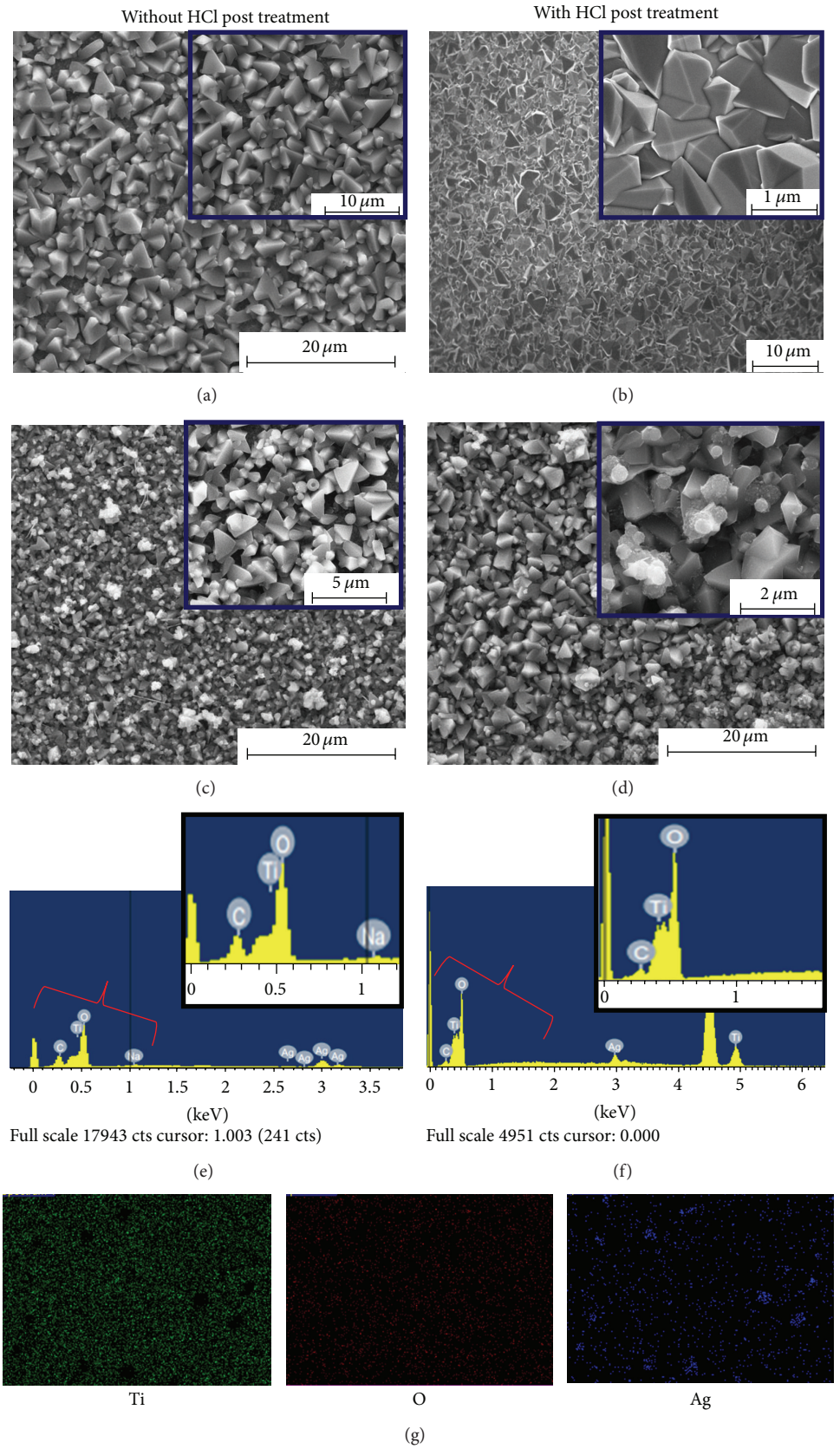

Figure 5: FESEM images of (a) TiO_2, (b) P-TiO_2, (c) Ag/TiO_2, and (d) P-Ag/TiO_2. EDX analysis of (e) Ag/TiO_2 and (f) P-Ag/TiO_2. (g) Element mapping of P-Ag/TiO_2.

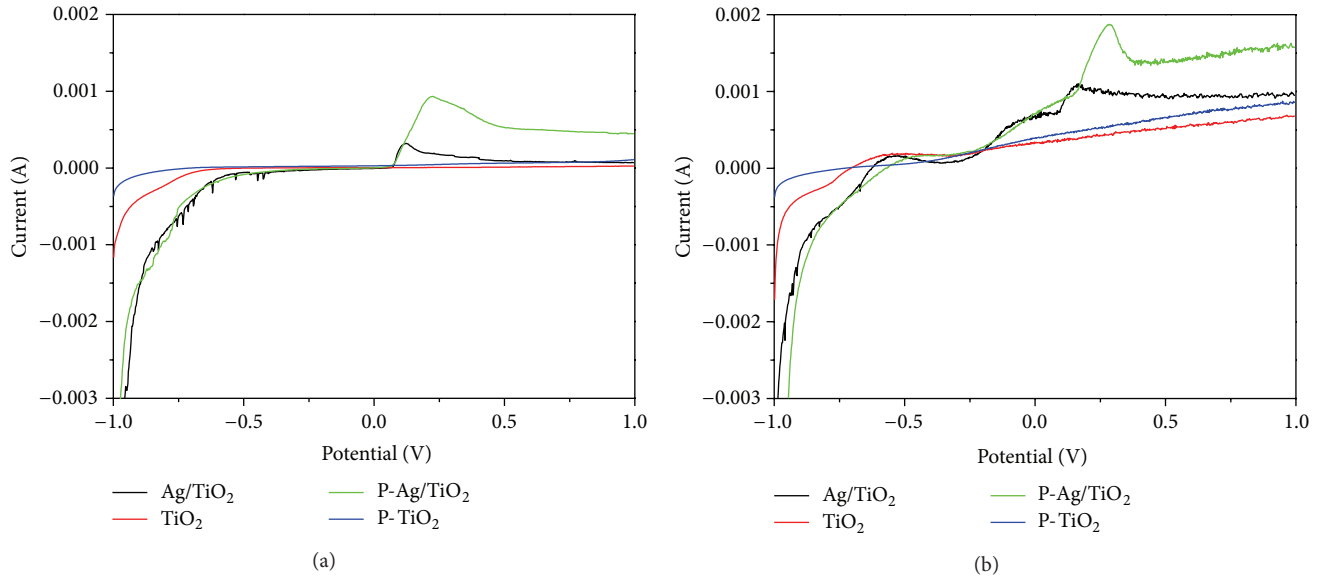

Figure 6: LSV voltammograms of TiO_2, Ag/TiO_2, $P\text{-}TiO_2$, and $P\text{-}Ag/TiO_2$ in (a) dark and (b) solar light, at a scan rate of 0.1 V/s.

film [39, 40]. After HCl posttreatment, the Na peak disappears. The C peak, found in the spectra of both treated and untreated films, may come from the residual carbon of the precursor solution such as unhydrolysed alkoxide or hydrocarbon groups from the surrounding environment, possibly created during the sample handling process. It is observed that the C content decreases after HCl posttreatment. This is most likely due to the removal of the Na. Na^+ will normally absorb CO_2 in air to form sodium carbonate and cause an increase in the amount of carbon. However, sodium carbonate will dissolve easily in HCl solution to form sodium chloride, CO_2, and H_2O. The residue sodium and chloride were then removed by rinsing with deionised water and ethanol. The areas of bright contrast on the element mapping correlate with the Ti, Ag, and O signal maps for $P\text{-}Ag/TiO_2$ shown in Figure 5(g).

LSV was conducted to study the redox properties of the samples. Figures 6(a) and 6(b) show the LSV voltammograms of the samples in darkness and under solar illumination. The results show that the photocurrent increases linearly with the potential in the low potential region and then remains constant. Oxidative peaks at around 0.22 V for the Ag/TiO_2 and $P\text{-}Ag/TiO_2$ films in the dark and under solar light suggest the presence of Ag with an oxidation state of O [41], corresponding to the reaction $Ag \rightarrow Ag^+ + e$. This suggests that the Ag on the surface of Ag/TiO_2 can be oxidised electrochemically [42]. Hence, we can conclude that Ag particles grow on TiO_2 thin films, not Ag^+ or Ag^{2+} ions. From the voltammogram, it could be observed that the current for TiO_2 and Ag/TiO_2 films, with and without HCl posttreatment, was enhanced under solar illumination compared to the current in darkness.

To examine the photocurrent activity of the films, the photocurrent profiles were measured against time. First, the influence of the loading concentration of Ag^+ on the photocurrent density was studied. As shown in Figure 7(a), the optimum concentration of Ag^+ is 0.005 M. This result indicates that the Ag loading concentration has an important effect on the photoelectrochemical activity as it generates free carriers or electron trapping sites. Increasing the concentration of Ag^+ to 0.01 M would decrease the photocurrent density because of the negatively charged Ag nanoparticles on the TiO_2 film that result from the Schottky barrier. The Schottky barrier is the potential barrier formed at the Ag/TiO_2 interface. It becomes dominant and retards the electron transport in the conduction bands. Consequently, the empty photoholes on the TiO_2 surface may become trapped by the high extent of negatively charged Ag particles before they have a chance react with others [41]. A decrease in the concentration would cause the photocurrent density to decrease due to the smaller amount of Ag acting as the electron acceptor [43].

The current responses of the TiO_2 and Ag/TiO_2 films at 0 V potential, with and without HCl posttreatment, are shown in Figure 7(b). The photocurrent densities for TiO_2 and Ag/TiO_2 are 178.63 $\mu A/cm^2$ and 430.33 $\mu A/cm^2$, respectively, while the HCl post-treated films $P\text{-}TiO_2$ and $P\text{-}Ag/TiO_2$ have photocurrent density of 197.18 $\mu A/cm^2$ and 933.30 $\mu A/cm^2$, respectively. By depositing Ag onto the TiO_2 thin film without HCl posttreatment, the photocurrent increased approximately 2.5-fold. The photocurrent density enhancement of as high as fivefold is achieved when Ag is deposited onto the TiO_2 thin film after posttreatment. These significant enhancements of photocurrent density are most probably due to the posttreatment of the TiO_2 thin film with HCl, which is essential to remove impurities such as Na. On the other hand, in presence of Ag, the TiO_2 thin film can effectively transfer photoelectrons and restrict the recombination of photoexcited electron-hole pairs.

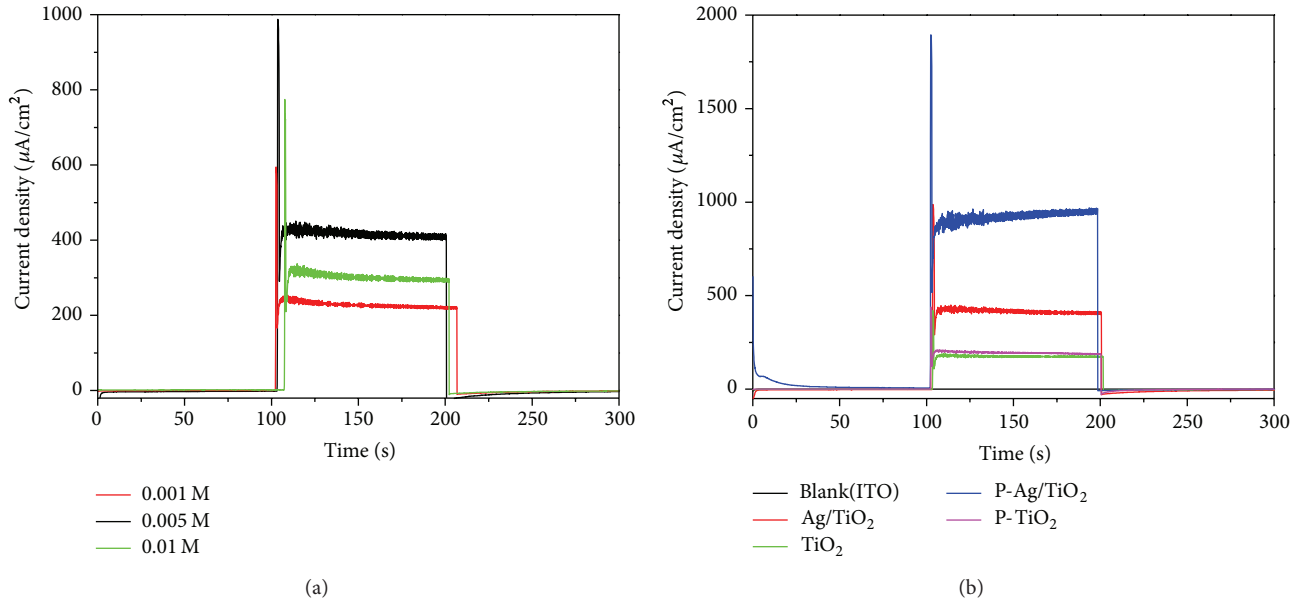

Figure 7: Photocurrent profile of (a) different concentrations of Ag^+ on TiO_2 and (b) ITO, TiO_2, Ag/TiO_2, $P\text{-}TiO_2$, and $P\text{-}Ag/TiO_2$.

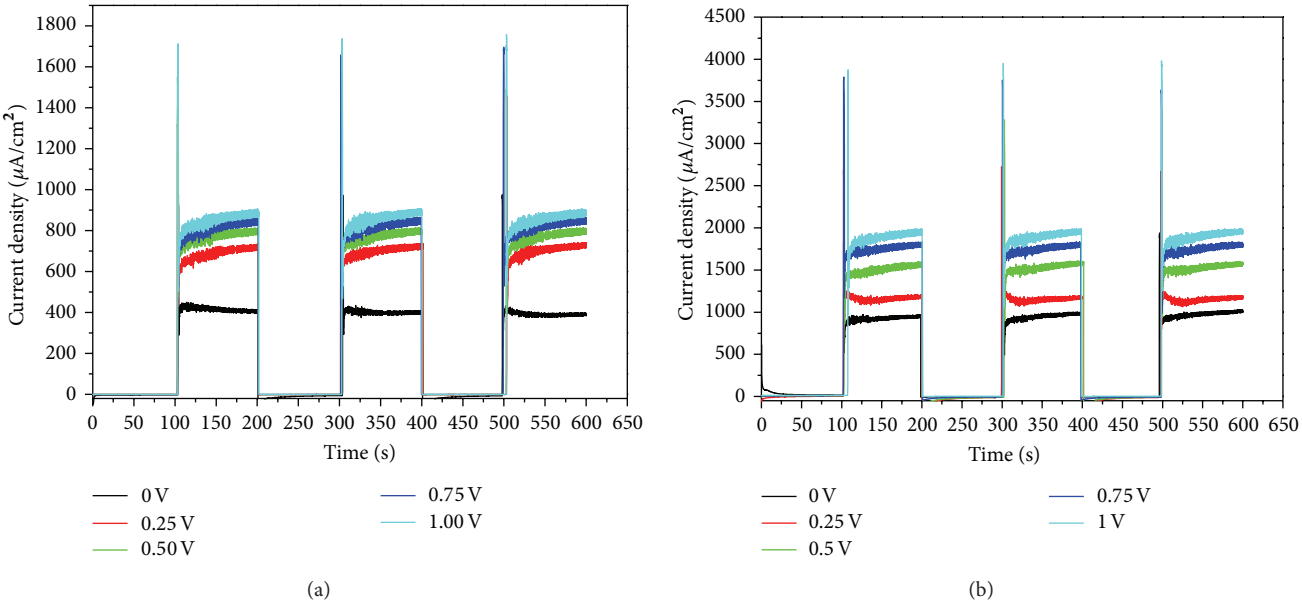

Figure 8: Photocurrent profile of (a) Ag/TiO_2 and (b) $P\text{-}Ag/TiO_2$ at various applied bias voltages under solar illumination.

The photocurrent responses of Ag/TiO_2 and $P\text{-}Ag/TiO_2$ under solar illumination are shown in Figures 8(a) and 8(b). As illumination began, there was a significant increase in the photocurrent and a photocurrent spike was observed. This phenomenon is likely due to the surface recombination process [44–48]. After the sudden increase in photocurrent after illuminating the film, a fast decay is observed which is likely attributed to accumulation of photogenerated holes on the surface of Ag/TiO_2 films which in turn allows their recombination with photogenerated electrons [45]. No current was produced when the light was turned off, even at the highest applied potential 1 V. There were excellent reproducibility and repeatability of results. This indicates that there is no photodegradation of the sample and the response is not affected by photooxidisable surface species [49].

The operation principle of the DSSC is based on photoexcitation of the dye, followed by electron injection into the conduction band of the TiO_2 surface. Figure 9(c) shows a schematic diagram of the operation principles of a DSSC based on an Ag/TiO_2 thin film. During solar irradiation, the dye absorbs incident light and promotes electrons to the excited state. The excited electron is injected into the conduction band of the TiO_2 particle. The dye is then oxidised by receiving the electron from the electrolyte through the

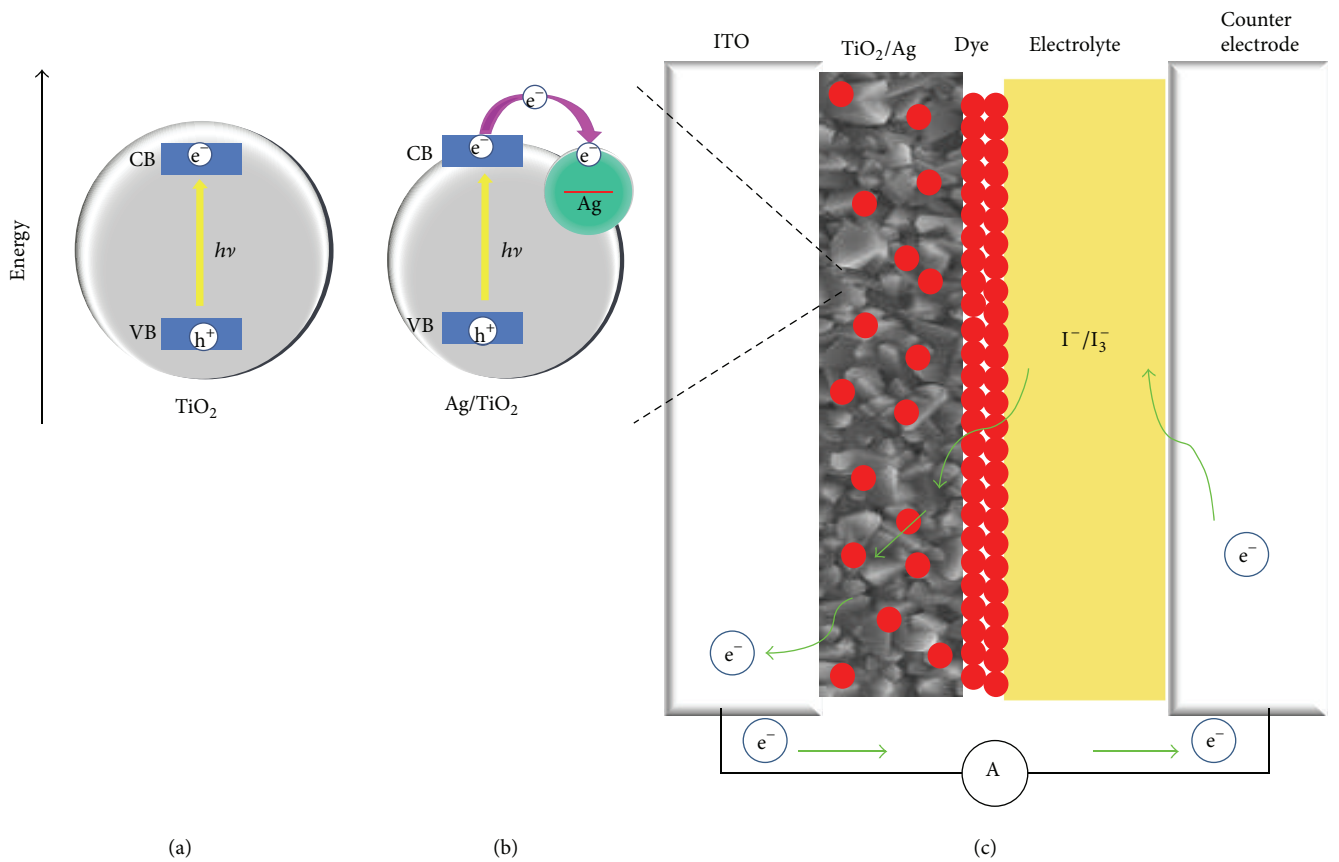

FIGURE 9: (a) Energy level diagram of TiO_2, (b) transfer of charge of Ag/TiO_2, and (c) schematic of the operation principles of the DSSC based on an Ag/TiO_2 thin film.

redox system and is ready to be used again. The electrolyte itself will regenerate via the platinum counter electrode by an electron passed through the external circuit. In our study, the deposition of Ag onto the TiO_2 thin film (Figures 9(a) and 9(b)) resulted in a change in the Fermi energy level; thus the electron in the conduction band of TiO_2 can be effectively captured by the Ag until the Fermi level equilibrium is obtained. This migration of generated electrons to Ag increases the lifetime of the holes and suppresses the electron-hole recombination, which is beneficial to photoelectrochemical activity. Without the threat of electron-hole recombination, the valence holes will then oxidise water and form hydroxyl radicals. These hydroxyl radicals will eventually react with water and degrade organic matters efficiently.

To examine the improvement in the efficiency as a result of the proposed posttreatment with HCl and surface modification by deposition of Ag, we measured the density-voltage (J-V) curves, which are shown in Figure 10. From analysis of the J-V curves, the critical parameters of the cell, such as open circuit voltage (V_{oc}), short circuit photocurrent density (J_{sc}), and the cell's fill factor (FF), can be obtained from the following equation [10]:

$$\mathrm{FF} = \frac{V_m J_m}{V_{oc} J_{sc}}, \tag{1}$$

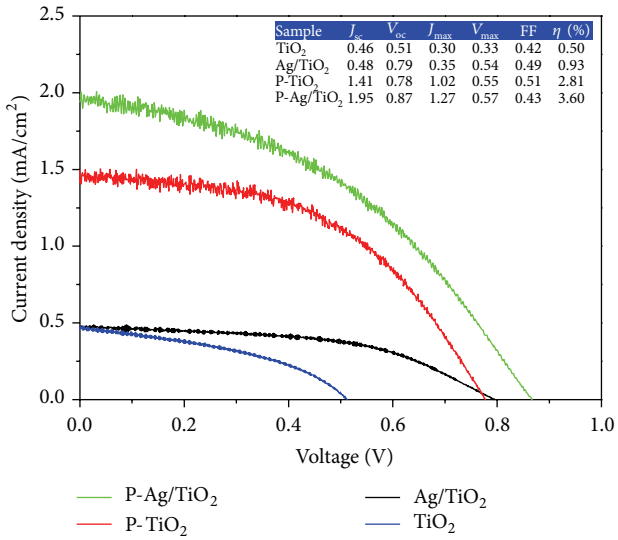

FIGURE 10: Density-voltage (J-V) curves of TiO_2, Ag/TiO_2, P-TiO_2, and P-Ag/TiO_2.

where V_m and J_m are the voltage and current densities, respectively, at maximum power output, respectively. The

cell's overall energy conversion efficiency (η) is estimated as follows:

$$\eta = \frac{V_{oc} J_{sc} FF}{I_s}, \quad (2)$$

where I_s is the intensity of the incident light. The results are summarised in the inset of Figure 10. The power conversion efficiency (η) of the Ag/TiO_2 film increased to 0.93%, compared with that of the TiO_2 thin film (0.50%). Following HCl posttreatment, the power conversion efficiency drastically increased to 2.81%, and the conversion efficiency of P-Ag/TiO_2 improved to 3.60%. The improvements are approximately twofold after deposition of Ag onto the TiO_2 thin film, approximately sixfold after HCl posttreatment, and approximately sevenfold after HCl posttreatment and Ag deposition. In previous studies, it was confirmed that sodium ions are detrimental to the photoactivity. Even at low concentrations, sodium could produce surface and bulk recombination centres of photogenerated electron-hole pairs and hence retard the photoefficiency of TiO_2 [50]. Therefore, after treatment with HCl to remove the sodium, the conversion efficiency was significantly enhanced. All Ag doped DSSCs exhibited better conversion efficiency. Moreover, the film subjected to both HCl posttreatment and Ag deposition showed the highest power conversion efficiency, almost sevenfold higher than that of the untreated film. This may be due to the synergetic effects of the removal of the sodium ion and the incorporation of silver.

4. Conclusion

We first reported on the DSSC performance of mixed rutile-anatase phase TiO_2 thin films produced by the AACVD method. This was followed by deposition of Ag nanoparticles onto the film through a simple sonochemical method. It has been shown that the photoelectrochemical properties and DSSC performance of the hybrid film were greatly enhanced following HCl posttreatment. The photocurrent measurements revealed good photocurrent response for the Ag/TiO_2 thin film. The photocurrent density of 933.30 $\mu A/cm^2$, with high stability, is an indication that the as-synthesised thin film is a potential candidate for solar energy conversion applications. A conversion efficiency of 3.63% has been achieved, with J_{sc}, V_{oc}, and FF of 1.95 mA/cm^2, 0.87 V, and 0.43, respectively, owing to the reduced band gap energy and retarded charge recombination, which were contributing factors to the improved photoelectrochemical and DSSC performance.

Conflict of Interests

The authors declare that there is no conflict of interests regarding the publication of this paper.

Acknowledgments

This work was supported by the University of Malaya Research Grant (RG197/11AFR), Science Fund from the Ministry of Science, Technology and Innovation (06-01-04-SF1513), and a High Impact Research Grant from the Ministry of Higher Education of Malaysia (UM.C/625/1/HIR/MOHE/05).

References

[1] H. Chang, H.-T. Su, W.-A. Chen et al., "Fabrication of multilayer TiO_2 thin films for dye-sensitized solar cells with high conversion efficiency by electrophoresis deposition," *Solar Energy*, vol. 84, no. 1, pp. 130–136, 2010.

[2] C. Edusi, G. Hyett, G. Sankar, and I. P. Parkin, "Aerosol-assisted CVD of titanium dioxide thin films from methanolic solutions of titanium tetraisopropoxide; substrate and aerosol-selective deposition of rutile or anatase," *Chemical Vapor Deposition*, vol. 17, no. 1–3, pp. 30–36, 2011.

[3] C.-S. Lee, J. Kim, G. H. Gu et al., "Photocatalytic activities of TiO_2 thin films prepared on Galvanized Iron substrate by plasma-enhanced atomic layer deposition," *Thin Solid Films*, vol. 518, no. 17, pp. 4757–4761, 2010.

[4] J. Gong, Y. Li, Z. Hu, Z. Zhou, and Y. Deng, "Ultrasensitive NH_3 gas sensor from polyaniline nanograin enchased TiO_2 fibers," *Journal of Physical Chemistry C*, vol. 114, no. 21, pp. 9970–9974, 2010.

[5] C. Wang, L. Yin, L. Zhang, Y. Qi, N. Lun, and N. Liu, "Large scale synthesis and gas-sensing properties of anatase TiO_2 three-dimensional hierarchical nanostructures," *Langmuir*, vol. 26, no. 15, pp. 12841–12848, 2010.

[6] P. Evans and D. W. Sheel, "Photoactive and antibacterial TiO_2 thin films on stainless steel," *Surface and Coatings Technology*, vol. 201, no. 22-23, pp. 9319–9324, 2007.

[7] C. W. Dunnill, Z. A. Aiken, A. Kafizas et al., "White light induced photocatalytic activity of sulfur-doped TiO_2 thin films and their potential for antibacterial application," *Journal of Materials Chemistry*, vol. 19, no. 46, pp. 8747–8754, 2009.

[8] R. S. Lima and B. R. Marple, "Thermal spray coatings engineered from nanostructured ceramic agglomerated powders for structural, thermal barrier and biomedical applications: a review," *Journal of Thermal Spray Technology*, vol. 16, no. 1, pp. 40–63, 2007.

[9] N. R. Mathews, M. A. C. Jacome, E. R. Morales, and J. A. T. Antonio, "Structural and spectroscopic study of the Fe doped TiO_2 thin films for applications in photocatalysis," *Physica Status Solidi C*, vol. 6, no. 1, pp. S219–S223, 2009.

[10] B. O'Regan and M. Grätzel, "A low-cost, high-efficiency solar cell based on dye-sensitized colloidal TiO_2 films," *Nature*, vol. 353, no. 6346, pp. 737–740, 1991.

[11] M. Grätzel, "Dye-sensitized solar cells," *Journal of Photochemistry and Photobiology C*, vol. 4, no. 2, pp. 145–153, 2003.

[12] S. Agarwala, M. Kevin, A. S. W. Wong, C. K. N. Peh, V. Thavasi, and G. W. Ho, "Mesophase ordering of TiO_2 film with high surface area and strong light harvesting for dye-sensitized solar cell," *ACS Applied Materials and Interfaces*, vol. 2, no. 7, pp. 1844–1850, 2010.

[13] S. Hwang, C. Kim, H. Song, S. Son, and J. Jang, "Designed architecture of multiscale porous TiO_2 nanofibers for dye-sensitized solar cells photoanode," *ACS Applied Materials and Interfaces*, vol. 4, no. 10, pp. 5287–5292, 2012.

[14] W. Weng, T. Higuchi, M. Suzuki et al., "A high-speed passive-matrix electrochromic display using a mesoporous TiO_2 electrode with vertical porosity," *Angewandte Chemie International Edition*, vol. 49, no. 23, pp. 3956–3959, 2010.

[15] Q. Zhang and G. Cao, "Nanostructured photoelectrodes for dye-sensitized solar cells," *Nano Today*, vol. 6, no. 1, pp. 91–109, 2011.

[16] M. N. An'amt, S. Radiman, N. M. Huang et al., "Sol-gel hydrothermal synthesis of bismuth-TiO_2 nanocubes for dye-sensitized solar cell," *Ceramics International*, vol. 36, no. 7, pp. 2215–2220, 2010.

[17] Y. Lee and M. Kang, "The optical properties of nanoporous structured titanium dioxide and the photovoltaic efficiency on DSSC," *Materials Chemistry and Physics*, vol. 122, no. 1, pp. 284–289, 2010.

[18] E. M. Jin, X. G. Zhao, J.-Y. Park, and H.-B. Gu, "Enhancement of the photoelectric performance of dye-sensitized solar cells using Ag-doped TiO_2 nanofibers in a TiO_2 film as electrode," *Nanoscale Research Letters*, vol. 7, no. 1, article 97, 2012.

[19] S. Lin, K. Lee, and J. Wu, "Plasmon-enhanced photocurrent in dye-sensitized solar cells," *Solar Energy*, vol. 86, no. 9, pp. 2600–2605, 2012.

[20] K. Prabakar, M.-K. Son, D. Ludeman, and H.-J. Kim, "Visible light enhanced TiO_2 thin film bilayer dye sensitized solar cells," *Thin Solid Films*, vol. 519, no. 2, pp. 894–899, 2010.

[21] B. Lei, Q. Luo, X. Yu, W. Wu, C. Su, and D. Kuang, "Hierarchical TiO_2 flowers built from TiO_2 nanotubes for efficient Pt-free based flexible dye-sensitized solar cells," *Physical Chemistry Chemical Physics*, vol. 14, no. 38, pp. 13175–13179, 2012.

[22] G. K. Mor, K. Shankar, M. Paulose, O. K. Varghese, and C. A. Grimes, "Use of highly-ordered TiO_2 nanotube arrays in dye-sensitized solar cells," *Nano Letters*, vol. 6, no. 2, pp. 215–218, 2006.

[23] S. Ito, T. N. Murakami, P. Comte et al., "Fabrication of thin film dye sensitized solar cells with solar to electric power conversion efficiency over 10%," *Thin Solid Films*, vol. 516, no. 14, pp. 4613–4619, 2008.

[24] L. Yan, F. Wu, L. Peng et al., "Photoanode of dye-sensitized solar cells based on a ZnO/TiO_2 composite film," *International Journal of Photoenergy*, vol. 2012, Article ID 613969, 4 pages, 2012.

[25] A. R. Malagutti, H. A. J. L. Mourão, J. R. Garbin, and C. Ribeiro, "Deposition of TiO_2 and Ag:TiO_2 thin films by the polymeric precursor method and their application in the photodegradation of textile dyes," *Applied Catalysis B*, vol. 90, no. 1-2, pp. 205–212, 2009.

[26] C. Su, L. Liu, M. Zhang, Y. Zhang, and C. Shao, "Fabrication of Ag/TiO_2 nanoheterostructures with visible light photocatalytic function via a solvothermal approach," *CrystEngComm*, vol. 14, no. 11, pp. 3989–3999, 2012.

[27] J. He, I. Ichinose, T. Kunitake, and A. Nakao, "In situ synthesis of noble metal nanoparticles in ultrathin TiO_2-gel films by a combination of ion-exchange and reduction processes," *Langmuir*, vol. 18, no. 25, pp. 10005–10010, 2002.

[28] F. Meng and Z. Sun, "A mechanism for enhanced hydrophilicity of silver nanoparticles modified TiO_2 thin films deposited by RF magnetron sputtering," *Applied Surface Science*, vol. 255, no. 13-14, pp. 6715–6720, 2009.

[29] P. Peerakiatkhajorn, C. Chawengkijwanich, W. Onreabroy, and S. Chiarakorn, "Novel photocatalytic Ag/TiO_2 thin film on polyvinyl chloride for gaseous BTEX treatment," *Materials Science Forum*, vol. 712, pp. 133–145, 2012.

[30] X.-G. Hou, M.-D. Huang, X.-L. Wu, and A.-D. Liu, "Preparation and studies of photocatalytic silver-loaded TiO_2 films by hybrid sol-gel method," *Chemical Engineering Journal*, vol. 146, no. 1, pp. 42–48, 2009.

[31] Y. S. Jin, K. H. Kim, S. J. Park, H. H. Yoon, and H. W. Choi, "Nanostructured TiO_2 films for dye-sensitized solar cells prepared by the sol-gel method," *Journal of Nanoscience and Nanotechnology*, vol. 11, no. 12, pp. 10971–10975, 2011.

[32] M. Sun, W. Fu, H. Yang et al., "One-step synthesis of coaxial Ag/TiO_2 nanowire arrays on transparent conducting substrates: enhanced electron collection in dye-sensitized solar cells," *Electrochemistry Communications*, vol. 13, no. 12, pp. 1324–1327, 2011.

[33] H. Zhang, G. Wang, D. Chen, X. Lv, and J. Li, "Tuning photoelectrochemical performances of Ag/TiO_2 nanocomposites via reduction/oxidation of Ag," *Chemistry of Materials*, vol. 20, no. 20, pp. 6543–6549, 2008.

[34] R. Liu, P. Wang, X. Wang, H. Yu, and J. Yu, "UV- and visible-light photocatalytic activity of simultaneously deposited and doped Ag/Ag(I)-TiO_2 photocatalyst," *Journal of Physical Chemistry C*, vol. 116, no. 33, pp. 17721–17728, 2012.

[35] N. Alenzi, W.-S. Liao, P. S. Cremer et al., "Photoelectrochemical hydrogen production from water/methanol decomposition using Ag/TiO_2 nanocomposite thin films," *International Journal of Hydrogen Energy*, vol. 35, no. 21, pp. 11768–11775, 2010.

[36] X. Cheng, Y. Xu, S. Gao, H. Zhao, and L. Huo, "Ag nanoparticles modified TiO_2 spherical heterostructures with enhanced gas-sensing performance," *Sensors and Actuators B*, vol. 155, no. 2, pp. 716–721, 2011.

[37] F. Hossein-Babaei, "Porous silver-TiO_2 Schottky-type chemical sensor fabricated on thermally oxidised titanium," *Electronics Letters*, vol. 44, no. 2, pp. 161–162, 2008.

[38] S. S. Samal, P. Jeyaraman, and V. Vishwakarma, "Sonochemical coating of Ag-TiO_2 nanoparticles on textile fabrics for stain repellency and self-cleaning—the Indian scenario: a review," *Journal of Minerals & Materials Characterization & Engineering*, vol. 9, no. 6, pp. 519–525, 2010.

[39] J. Liang, Y. Feng, G. Liang et al., "Effects of post-treatment on the photocatalytic activity of mesoporous TiO_2 thin films," *Journal of Materials Science Letters*, vol. 22, no. 21, pp. 1503–1506, 2003.

[40] J. C. Yu, J. Yu, and J. Zhao, "Enhanced photocatalytic activity of mesoporous and ordinary TiO_2 thin films by sulfuric acid treatment," *Applied Catalysis B*, vol. 36, no. 1, pp. 31–43, 2002.

[41] J. Zheng, H. Yu, X. Li, and S. Zhang, "Enhanced photocatalytic activity of TiO_2 nano-structured thin film with a silver hierarchical configuration," *Applied Surface Science*, vol. 254, no. 6, pp. 1630–1635, 2008.

[42] I. Boskovic, S. V. Mentus, and M. Pjescic, "Electrochemical behavior of an Ag/TiO_2 composite surfaces," *Electrochimica Acta*, vol. 51, no. 14, pp. 2793–2799, 2006.

[43] G. Li, T. Wang, Y. Zhu et al., "Preparation and photoelectrochemical performance of Ag/graphene/TiO_2 composite film," *Applied Surface Science*, vol. 257, no. 15, pp. 6568–6572, 2011.

[44] L. M. Abrantes and L. M. Peter, "Transient photocurrents at passive iron electrodes," *Journal of Electroanalytical Chemistry and Interfacial Electrochemistry*, vol. 150, no. 1, pp. 593–601, 1982.

[45] M. Bledowski, L. Wang, A. Ramakrishnan et al., "Visible-light photocurrent response of TiO_2-polyheptazine hybrids: evidence for interfacial charge-transfer absorption," *Physical Chemistry Chemical Physics*, vol. 13, no. 48, pp. 21511–21519, 2011.

[46] A. Hagfeldt, H. Lindström, S. Södergren, and S.-E. Lindquist, "Photoelectrochemical studies of colloidal TiO_2 films: the effect of oxygen studied by photocurrent transients," *Journal of Electroanalytical Chemistry*, vol. 381, no. 1-2, pp. 39–46, 1995.

[47] P. Salvador, M. L. G. González, and F. Muñoz, "Catalytic role of lattice defects in the photoassisted oxidation of water at (001) n-titanium(IV) oxide rutile," *Journal of Physical Chemistry*, vol. 96, no. 25, pp. 10349–10353, 1992.

[48] D. Tafalla, P. Salvador, and R. M. Benito, "Kinetic approach to the photocurrent transients in water photoelectrolysis at n-TiO_2 electrodes. II. Analysis of the photocurrent-time dependence," *Journal of the Electrochemical Society*, vol. 137, no. 6, pp. 1810–1815, 1990.

[49] R. Passalacqua, C. Ampelli, S. Perathoner, and G. Centi, "Anodically formed TiO_2 thin films: evidence for a multiparameter dependent photocurrent-structure relationship," *Nanoscience and Nanotechnology Letters*, vol. 4, no. 2, pp. 142–148, 2012.

[50] Y. Paz and A. Heller, "Photo-oxidatively self-cleaning transparent titanium dioxide films on soda lime glass: the deleterious effect of sodium contamination and its prevention," *Journal of Materials Research*, vol. 12, no. 10, pp. 2759–2766, 1997.